Year 3 MEng Project
Thesis

Measurement of Periodic Photodiode Breakdown

Lyudmil Vladimirov (ID 200791658)

Supervised by Dr John Marsland

April 30, 2014

Abstract

Avalanche photodiodes are a primary part of photon counting systems which are used in a wide range of applications, such as long distance optical communication and quantum cryptography. In this paper, the time-dependent behaviour of Single Photon Avalanche Diodes (SPADs), using a Bias Tee circuit for quenching, will be studied. The Bias Tee shall allow for the combination of a DC and an AC signal to be applied, which will cause the biasing voltage of the SPAD to oscillate above and below the breakdown point, thus enabling and disabling the device once per period of the applied AC signal. The two maximum Photon Detection Rates of using the same SPAD device within a Passive Quenching Circuit and the developed Bias Tee Quenching circuit, respectively, will be identified, reported and compared. To the best of our knowledge, this is the first report of a Bias Tee circuit being used as a quenching technique for SPADs.

Contents

List of Figures

List of Tables

List of Notation

f_{AC}	Frequency of the applied AC signal
f_c	Cut-off frequency
R_L	Load/Quenching Resistor
R_{SPAD}	Internal Resistance of SPAD
R_S	Sensing Resistor
V_A	Applied Bias Voltage
V_B	Reverse Breakdown Voltage
V_E	Excess Bias Voltage
AC	Alternating Current
APD	Avalanche Photo Diode
AQC	Active Quenching Circuit
BTQC	Bias Tee Quenching Circuit
C	Capacitance (F)
DC	Direct Current
DCR	Dark Count Rate
L	Inductance (H)
PDP	Photon Detection Probability
PDR	Photon Detection Rate

PMT Photo-Multiplier Tube

PQC Passive Quenching Circuit

R Resistance (Ω)

RF Radio Frequency

SPAD Single-Photon Avalanche Diode

Chapter 1

Project Specification Report [1]

Avalanche photodiodes (APDs) have a characteristic breakdown voltage in reverse bias above which the steady state current is limited only by the external resistance. APDs can be biased above the breakdown voltage for very short periods of time whilst the avalanche current increases. This project will use a bias tee circuit to combine DC and AC voltages that, when applied to the APD, will drive the APD into reverse breakdown once per period of the AC component. Then the time dependence of the avalanche current will be measured using an oscilloscope at the highest frequency range allowed by the system. The main challenges of this project are (i) high frequency operation and (ii) controlling the light incident on the APD and excluding ambient light sources. If the light incident on the APD can be reduced to very low levels then it may be possible to bias the APD continuously above the breakdown voltage and operate in so called photon counting mode.

(NOTE: The initial Gantt Chart of the projects estimated progress can be seen in Fig. A.1 of the Appendix)

Chapter 2

Introduction[1]

In recent years, an increased interest in high-sensitivity sensing of optical signals in environments with low light intensity, has been observed. Under such conditions, using conventional PIN photodetectors which linearly convert the received optical signal into an equivalent current signal has proven to be inefficient. The reason for this is that, due to the small internal gain of the device, the out-putting current coming from the implementation of such devices has a significantly small amplitude. This fact then gives birth to the necessity of using complex and costly amplifier circuits, in order to bring the output current to a detectable amplitude. However, the introduction of such amplifier blocks also leads to the introduction of considerably disruptive noise, which is added to the already overwhelming Johnson noise arising from resistive elements in the detector itself .

A common approach which strives to eliminate this problem is based on the implementation of a non-linear detection scheme, according to which the detection of a photon results in the production of a relatively high, saturated current that can be detected easily and without ambiguity by an electronic circuitry. Single photon avalanche diodes (SPAD's) provide this means of non-linear conversion by exploiting the impact ionization effect, which provides an internal avalanche multiplication gain. This internal gain provided by the device itself, automatically improves the signal-to-noise ratio and eliminates the necessity for an amplifier at the output. Ever since they were initially developed, SPAD's have been thoroughly investigated and improved [4][7][8][9]. Over the past few years, considerable progress has been achieved in the design and fabrication of Si and InGaAs/InP SPAD's and devices with good characteristics and reliable operation have been made commercially available.

When designing circuits for single photon detection using SPADs, what is of great interest is the choice of an appropriate quenching circuit to enable detection of consequently arriving photons. These quenching circuits are used to reset the SPAD after a photon is detected and their characteristics have the greatest effect on the timing constraints of the overall detector circuit. The generic categories of quenching circuits are two, passive and active. Passive quenching circuits are essentially implemented by adding a passive component, such as a resistor, in series with the SPAD.

A useful approach for designing passive quenching circuitry of SPADs is presented in [10]. Furthermore, passive quenching circuits have been studied in [11], [5] and [12] proving their simplicity and demonstrating how their operation can even be simulated, with surprisingly high accuracy, using different model representations. Active quenching circuits use complex circuitry, involving both passive and active components, in order to provide the desired quenching. The circuit configuration for active quenching can vary from application to application depending on the requirements. A general purpose active quenching circuit, which allows for a counting rate of above 25 Mcounts/s and significantly reduces the afterpulsing effect is presented in [13]. Other active quenching circuits are also shown and their design considerations are studied in [5] and [14].

Although many research activities and studies about both passive and active quenching have been performed, little is known about the applicability of Bias Tee circuits as a means for quenching. In the past, such circuits have mainly been used in a wide range of communication applications to provide a combination of RF and DC signals for powering remote devices, when the use of two separate cables is considered unreliable. Bias Tees have also been used with photodiodes, but in a different configuration than what is intended for this project. Previous applications used the Bias Tee circuit between the output of the photodetector and the amplifier, in order to prevent the high frequency components of the signal from leaking into the common supply rail and conversely excluding any noise caused by the power supply. The main design considerations for designing Bias Tee circuits have been studied and presented in [15] and [16]. No research papers and no publications have been identified, where the Bias Tee circuit has actually been used to quench a SPAD, a fact which makes the concept of researching the specific area highly challenging.

2.1 Industrial relevance, real-world applicability and scientific/societal impact

During the past few years, there has been a significant increase in the sensor performance requirements coming from the world of experimental sciences in chemistry, biology and physics. What is more, market demands keep evolving and becoming more and more challenging. For example, cameras produced these days have to combine high resolution and frame rate, with extremely small packaging sizes for mobile applications. As it becomes obvious the necessity for development of unconventional imaging techniques, to cope with the modern technological evolution, is becoming increasingly high.

Single photon avalanche photodiodes (SPADs) have only been developed during recent years and, despite this fact, they have managed to replace conventional photomultiplier tubes (PMTs) in a wealth of applications. Although a number of disadvantages are involved in the use of SPADs instead of PMTs, such as dark count rate and slightly higher levels of noise, their immunity to magnetic fields, single photon response and high detection efficiency make the SPADs the number one choice. What is also remarkable is the fact that SPADs have a significantly lower price compared to PMTs, whose extremely complicated internal structure is mostly handmade, setting their price relatively high. Today SPADs are profitably used in a wide range of applications such as laser ranging, single molecule detection, fluid velocimetry, medical imaging, distributed sensing and application are even found in studies of high field properties of semiconductors.

Although SPADs have developed swiftly over the past few years, one issue which still remains is the fact that the timing performance of the actual photodetector depends on the characteristics of the Quenching circuit used. Passive Quenching Circuits (PQCs) have proven to be an effective circuit when it comes to testing and evaluation of SPAD devices, but only to that point. PQCs cannot be used in real life applications because they present relatively high afterpulsing and dead time, which in turn leads to significantly low counting rates. For this reason, when performance is critical, scientists need to employ one of the many different Active quenching circuits (AQCs) in order to satisfy their requirements. However, choosing the appropriate AQC for a given application can be a real struggle. AQCs may vary extensively from application to application and involve a great deal of complexity and for this reason their price is significantly higher than that of PQCs.

As a result, an emerging need for developing a cheaper, but in the same time competently reliable alternative circuit to AQCs arises. Due their relatively sim-

ple configuration, Bias Tee circuits could potentially be implemented instead of AQCs. If the quenching configuration, proposed in this project, is confirmed to present satisfyingly good timing characteristics, which can be compared to the ones achieved by AQCs, then their suitability to be used as Quenching circuits will be certified, a fact which can lead to the introduction of a completely new chapter in the history of SPAD quenching circuits. Considering the vast volume of applications that SPADs currently maintain in the modern technological world, such an innovation could be the stepping stone for a series of technological advancements. First of all, since Bias Tee circuits are significantly cheaper to produce than conventional AQCs, developing a technique to allow for their implementation instead of AQCs can potentially give rise to huge savings, allowing for money to be spent on the improvement of other components, rather than the quenching circuit itself. Furthermore, due to the remarkably lower complexity involved in the development of Bias Tees, the time required for this process will also be significantly reduced. This will give scientists the opportunity to spend more time on the enhancement of other aspects of their projects, or could lead to an overall reduction of the development process. Since modern business models evolve around money and time, it becomes fairly obvious how the potential outcomes of this project can have a positive impact on the evolution of SPAD related applications and the overall engineering industry as a whole.

Chapter 3

Theoretical Background[1]

3.1 Single Photon Avalanche Diodes

Single Photon Avalanche Diodes (SPADs), a.k.a. Geiger-mode Avalanche Diodes, are Avalanche Photo Diodes(APDs) specifically designed to operate continuously in Geiger mode. An APD is said to be operating in Geiger mode, when it's operational voltage bias exceeds the reverse breakdown limit of the device. Such devices demonstrate high levels of internal current gain by exploiting the impact ionisation and avalanche multiplication effects.

3.1.1 Structure

A general schematic cross section of fabricated Avalanche Photodiodes is presented in Fig 3.1. The shown p-tub guard rings surrounding the p+ implantation are used in order to avoid edge breakdown and thus reduce the risk of premature breakdown of the device. The p+ and n+ implantations will ensure a notably narrow depletion region, which in turn provides a remarkably high electric field across it. A high electric field is necessary, since it will increase the acceleration of generated carriers and will thus amplify the impact ionisation rate, producing an extremely high internal current gain. The section of the device denoted as the active area is implemented by the introduction of a small optical window in the metal coating of the device, which allows small amounts of photons to enter and diffuse across the region where avalanche multiplication occurs.

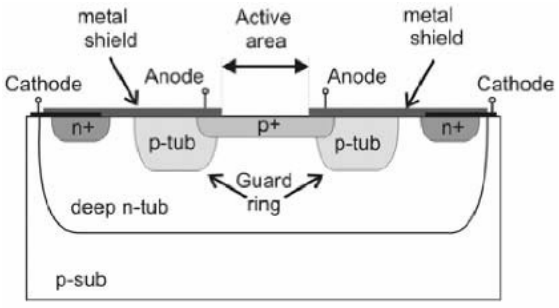

Figure 3.1: Basic structure of an APD cross section [2]

3.1.2 Operation

SPADs are essentially implemented as p-n junctions biased at a voltage V_A above the reverse breakdown voltage V_B. In this regime of operation, known as Geiger mode, the electric field is so high that photo-generated carriers are accelerated to such a degree that they start impact ionising. Impact ionisation is achieved when energetic -parent- charge carriers are given enough kinetic energy, such as to knock other -child- charge carriers out of their bound state and promote them to a conduction band state. This process leads to an avalanche multiplication and the creation of additional electron hole pairs . Fig 3.2 shows a general representation of the impact ionisation process.

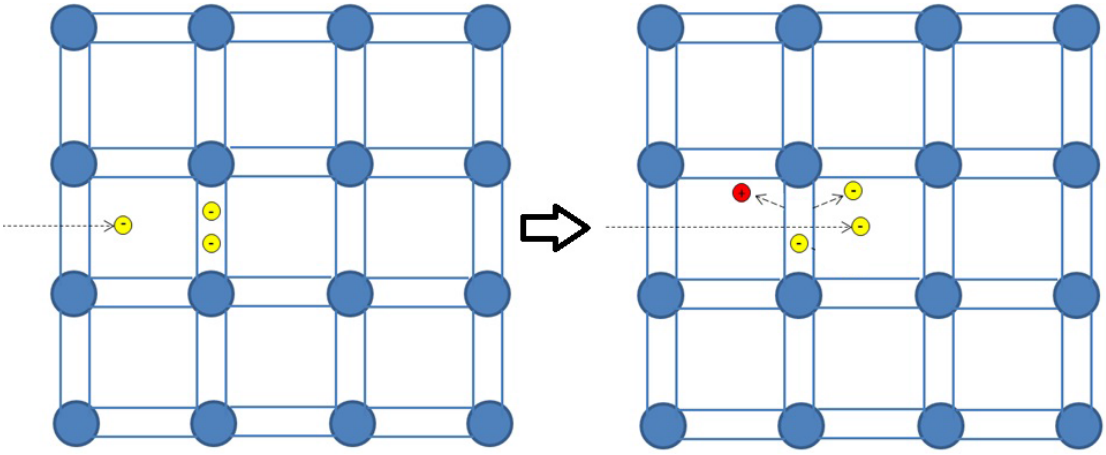

Figure 3.2: Representation of the impact ionization process. Each blue circle represents an atom in the semiconductor lattice and the two lines joining adjacent atoms represent a covalent bond comprising of two atoms. Yellow and red particles indicate electrons and holes, respectively.

An avalanche in the multiplication region causes an avalanche current to flow. This current rises swiftly, in a matter of micro or maybe even nanoseconds, until it reaches a measurable steady state in the milliampere range. If the initial carrier was photo-generated, then the leading edge of the avalanche pulse indicates the arrival time of a detected photon. Fig 3.3(a) shows a typical IV characteristic of APDs and Fig 3.3(b) identifies the different ranges of operation for common photodiodes, APDs and SPADs.

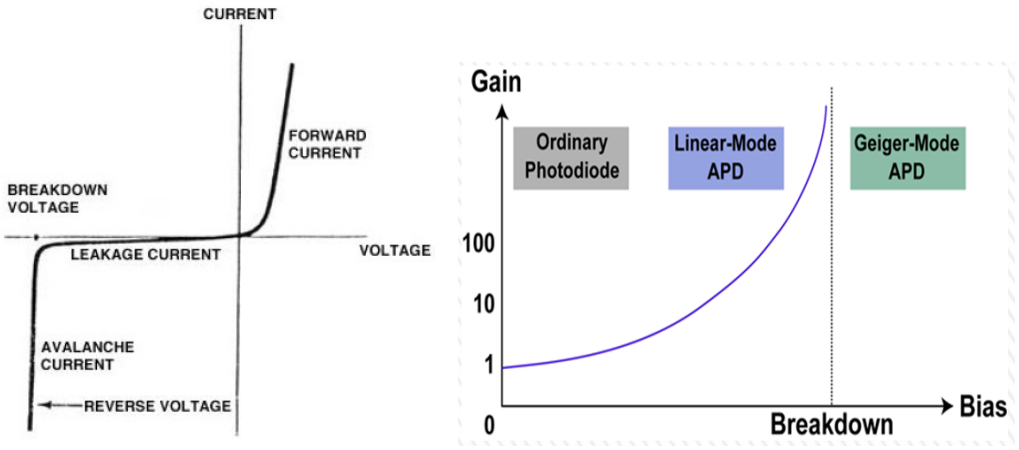

Figure 3.3: (a)Typical IV characteristics curve for APDs (b)Gain vs Voltage curve indicating the range of operation of each kind of photodiode [3]

3.1.3 Performance and Constraints

The noise performance of SPADs is mainly quantified in terms of spurious pulses in the dark, known as dark counts. Dark counts are characterised by a base frequency, known as the Dark Count Rate (DCR) and are caused by charge carriers being generated either thermally, or through tunnelling. The relative impact of both of the effects can be observed by a device analysis as a function of the Excess Bias Voltage $V_E = V_A - V_B$, where V_A is the applied bias and V_B is the reverse breakdown voltage of the device. Also, the breakdown voltage of the device (V_B), and thus the DCR, is dependent upon the temperature of the junction. Fig 3.4 and 3.5 show the dependence of DCR on the excess voltage and temperature, respectively. Fig 3.6 shows the relation between temperature and the breakdown voltage V_B of the device.

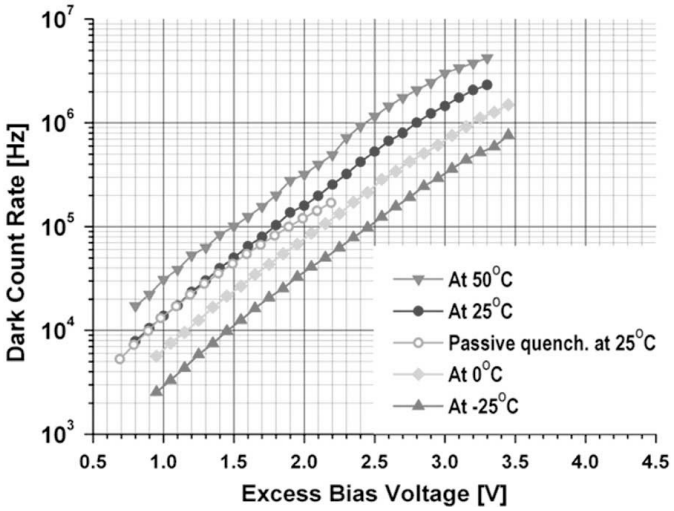

Figure 3.4: Dark count rate (DCR) as a function of excess bias voltage at four temperatures. [4]

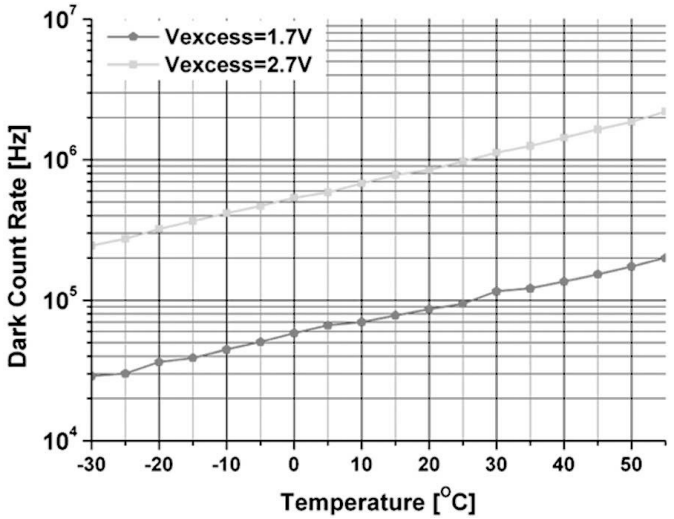

Figure 3.5: Dark count rate (DCR) as a function of temperature at two values of excess bias voltage [4]

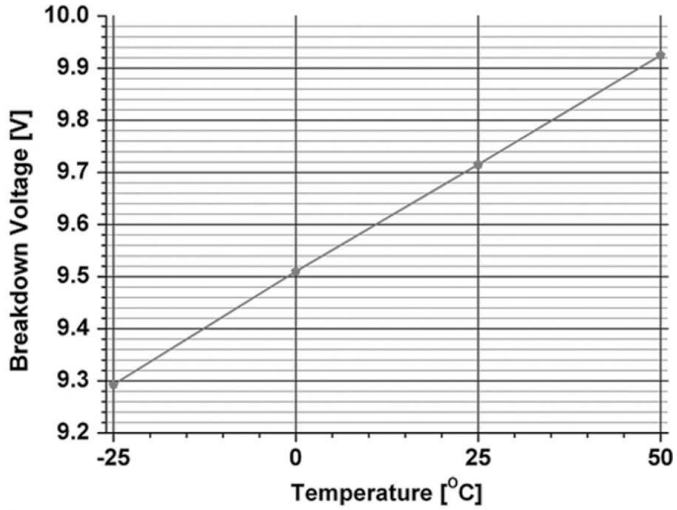

Figure 3.6: Breakdown voltage V_b as a function of temperature [4]

The sensitivity of SPADs is defined as the probability of a photon striking the lattice to cause an avalanche and thus create a current pulse. This attribute is called Photon Detection Probability (PDP) and is highly dependent on the excess bias voltage (V_A) applied to the device and the wavelength of the photon to be detected. Dark counts, as mentioned above, compete with photogenerated carriers in triggering an avalanche, thus reducing the overall sensitivity. Fig 3.7 shows a plot of the PDP at room temperature.

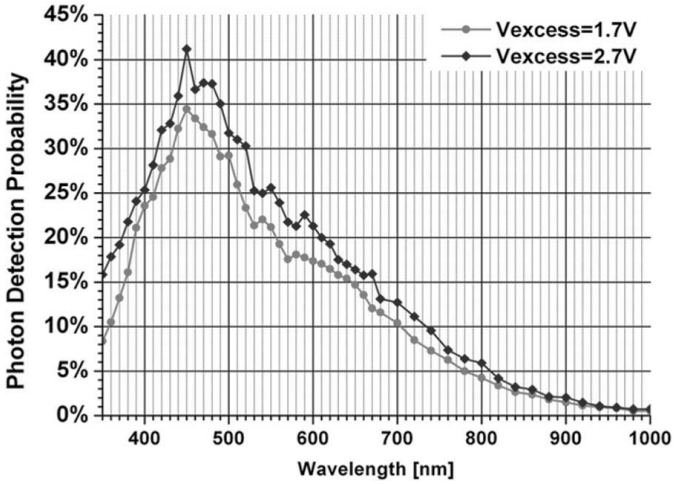

Figure 3.7: Photon detection probability(PDP) as a function of wavelength for two values of excess voltage. [4]

Afterpulsing also affects the sensitivity of a SPAD and is mostly present in PQCs. This phenomenon is caused by the release of electrons captured by trapping centers in the multiplication region, during previous Geiger pulses. The released electrons can potentially re-trigger a subsequent avalanche, producing a false current pulse on the output. The possibility of such an event taking place is characterized by the parameter named as Afterpulsing Probability. This parameter is determined by the number of carriers involved in the avalanche, which consequently is a function of the device's parasitic capacitance. Since one photon can generate on average more than one events, the maximum rate of detectable photons is most likely to be decreased. Fig 3.8 shows the phenomenon of afterpulsing expressed both in terms of the current and the voltage of the devices.

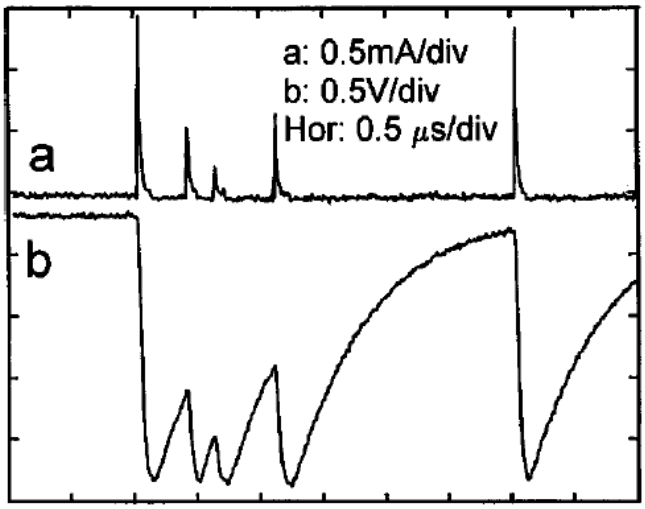

Figure 3.8: Re-triggering of a SPAD in a passive quenching circuit during the recovery transient after an avalanche pulse, which is the first one displayed on the left side. a) avalanche current Id, b) diode voltage Vd. [5]

The uncertainty of the time delay between the moment when a photon strikes the lattice and the moment when a pulse is displayed on the monitor is known in literature as timing resolution, or timing jitter. Depending on the size of the devices the timing jitter may depend on the time required for a photogenerated carrier to be absorbed by the multiplication region (for small devices) or may be caused by fluctuations on the avalanche propagation across the active area (for large devices).

3.2 Quenching Circuits

As explained in the previous section, at a voltage V_A above the breakdown voltage V_B, when a photon impinges the active area of a SPAD, it's energy is absorbed and the first electron-hole pair is introduced within the depletion region. These charge carriers then start a chain reaction, known as avalanche, creating even more charge carriers which are free to move. Thus, an avalanche current starts to flow, which, at some finite point, stabilises itself to a certain value of hundreds or thousands of micro amperes and the detection of the first photon is achieved.

However, this functionality on its own is not particularly useful, since it only allows for the detection of the first single photon. In order to achieve continuous single photon detection, the device needs to be reset, every time a photon is detected. More specifically, once an avalanche current -thus a photon- is detected, the applied voltage V_A across the device needs to be brought below the breakdown voltage V_B. Once this is done, the avalanche current created previously is stopped and the device is allowed to recover to its initial bias, above V_B, which enables it to detect a consequent photon. This functionality is mainly achieved through the use of either Passive or Active Quenching Circuits.

3.2.1 Passive Quenching Circuits

As implied by their name, Passive Quenching Circuits (PQCs) use passive components to achieve quenching of the avalanche circuit. The most common approach is implemented by including a resistor in series with the SPAD. Fig. 3.9 shows the schematic of a typical PQC and also illustrates the voltage and current change across the diode when a photon is detected. Once the avalanche current starts rising, the voltage across the ballast(or load) resistor R_L also increases which leads to a reduction of the voltage V_A across the device. Once the voltage of the resistor is sufficiently high to force the device below breakdown, the avalanche current is stopped. Continuing, the device will slowly start to recharge, until the appled voltage is returned to it's original value. The sensing resistor R_S is present to enable the triggering of the comparator.

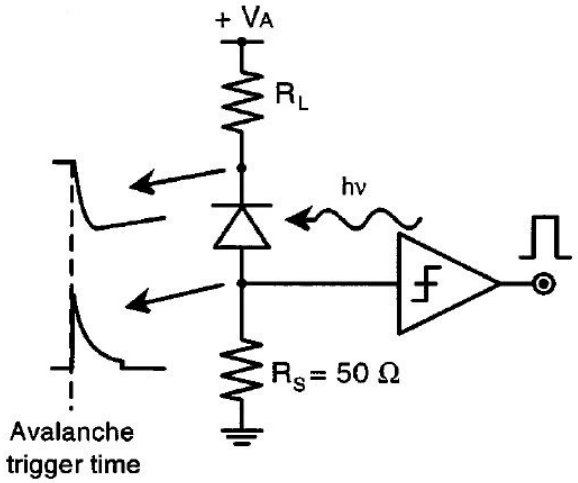

Figure 3.9: Typical passive quenching configuration for current sensing. The avalanche signal is sensed by the comparator that produces a standard signal for pulse counting and timing. [5]

Despite the fact that passive quenching is relatively simple, there exist a significant number of drawbacks associated with it's operation. First and foremost, is the duration of the recharge time, or otherwise called dead time. In this quenching arrangement, the dead time can be in the order of several μs, which automatically limits the maximum photon counting rate to a few thousand counts per second. In addition to this fact, the actual dead time of the device itself is not well defined and there is a great amount of uncertainty associated with it. These two disadvantages themselves are sufficient to pose serious problems for a number of applications.

Additional drawbacks are introduced to this configuration because of the amplitude that the avalanche current is allowed to reach, before it is successfully quenched. Due to it's high magnitude, this current dissipates significant amounts of energy in the device, which leads to an escalation of the junction's temperature. This, in turn, leads to an increase of the Dark Count Rate, which is the main source of noise for the device. (see Section 3.1.3) One further drawback, caused by the amplitude of the avalanche current, is the intensity of afterpulsing. Since the current is high, more charge carriers pass through the depletion region for a given time and thus the overall amount of trapped charge carriers is increased. These carriers will only be released later in the process, and can most certainly create additional (faulty) avalanches.

The limitations which are set to a SPAD in passive quenching circuits can make

it highly unsuitable for a wide range of applications. For this reason, another quenching configuration needs to be devised, which shall minimise the drawbacks mentioned above. This is reason why Active Quenching Circuits (AQCs) become increasingly important.

3.2.2 Active Quenching Circuits

Unlike PQCs, Active Quenching Circuits (AQCs) are a complex set of circuitry, devised specifically to by-pass the disadvantages posed by the formerly mentioned circuit. Depending on the nature of the application for which the SPAD needs to be used, AQCs can be designed accordingly to optimize specific features of it's operation.

Fig.3.10 shows an example of a Geiger mode AQC. Essentially, it is a combination of passive and active quenching circuits. When an incident photon strikes the surface of the device and starts the avalanche current, the AQC will quickly sense the current and reduce the voltage of the device below breakdown. After a certain hold off time, which is also controlled by the capacitor VC at the input of the comparator, the voltage bias of the junction will be subsequently restored. Unlike the previous example, this time the current will be ceased as soon as it is detected, rather than left to saturate to a finite point, governed by the external resistance. As a consequence, power dissipation across the device will be reduced, thus providing lower DCR and significantly diminished Afterpulsing. By implementing this configuration, the maximum counting rate of the circuit in this example is also increased to 10 Mcounts/s.

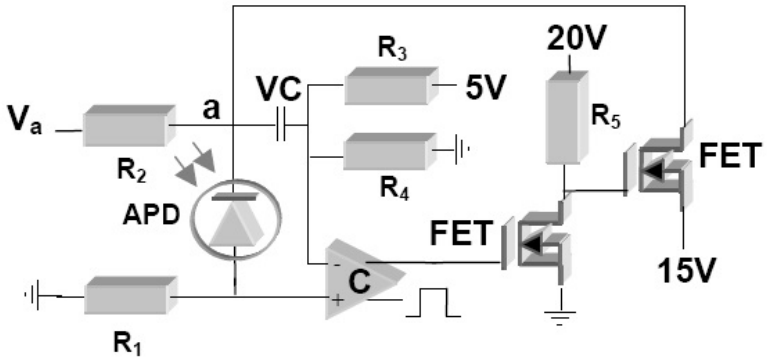

Figure 3.10: Example active quenching circuit, which allows swift sensing and reduction of the avalanche current. [2]

Evidently, the advantages and improvements that AQCs can offer are numerous and for this reason they have replaced the traditional PQCs in a wide range of applications. However, the complexity of such circuits and their strong dependence on the SPAD used, makes them significantly hard to design and implement.

3.2.3 Bias Tee Circuits

Bias Tee (or Bias-t) circuits are three port devices, which allow the combination of DC and RF signals to set the bias of electronic components. Such circuits are commonly used in telecommunications as diplexers, to prevent inter-modulation and minimise the reflected power. Generally, they are implemented as a high pass and a low pass filter, joined in parallel. A typical Bias Tee is shown in Fig 3.11. This configuration, allows the addition of the RF and DC signals on the output port, while simultaneously isolating the two signals from each other.

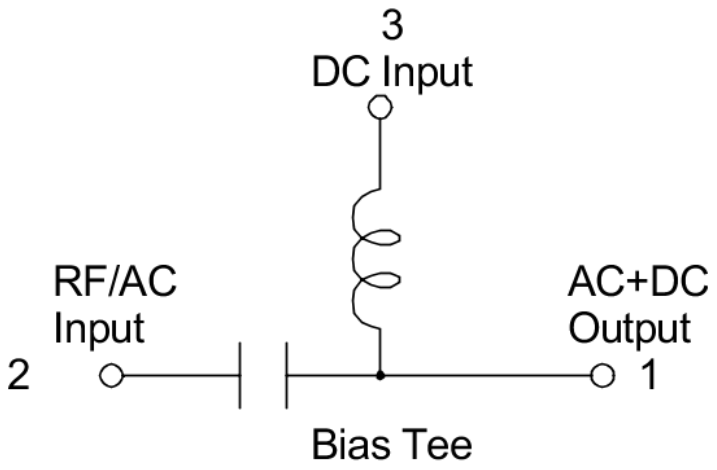

Figure 3.11: Schematic of a typical Bias-t circuit. [6]

Due to it's above mentioned property, the Bias Tee circuit could potentially be used for quenching. If the SPAD's cathode is connected to the ground and it's anode is placed at the output of the Bias Tee, the bias voltage of the junction will be entirely dependent on the voltages applied at the input. Then, having the DC input set at the breakdown voltage of the device, the AC signal will force the device above and below breakdown, once per period. This means that, during the positive cycle of the RF signal, the SPAD will be enabled to detect a photon and

when the RF enters it's negative cycle, the avalanche current will be ceased. As soon as the next positive cycle occurs, the device will again be ready to detect another incident photon.

The classification of Bias Tee circuits as a Passive or Active Quenching Circuit cannot be clearly defined. The reason for this is that although the components of the circuit are passive, the means of altering the bias across the SPAD are active but, yet again, they do not depend on feedback received from the output. However, this configuration can prove to provide the optimal combination of the advantages offered by both passive and active quenching circuits. Although Bias Tee circuits are slightly more sophisticated than the traditional passive quenching configuration, their complexity is significantly lower than that of AQCs. Furthermore, the dead time of the device is no longer dependent on the parameters of the external passive components, while setting the correct amplitude and frequency of the RF signal, will ensure sufficient control over the avalanche current.

Chapter 4

Materials and Methodology

4.1 Materials/Equipment used[1]

The specific set of equipment used throughout the entire project is presented and described in Table (4.1).

Table 4.1: Equipment used throughout the project

Equipment	Description
Silonex SLD-70BG	Infrared Rejection Filter Planar Photodiode
Vishay BPW21R	Silicon Photodiode
Tektronix TDS1002C EDU	Oscilloscope
TOKO 10RB104K	100mH Inductors
Black Star JUPITER 2010	Function Generator

4.2 Methodology

4.2.1 Design of the Bias Tee circuit[1]

The most important component of the overall circuit is the Bias Tee. For this reason, this was the first component which was decided to be designed and tested. In order for this to be achieved, the exact values of the capacitor and the inductor inside the circuit needed to be calculated and set according to the requirements of the project. The intentions for this project were to use a 10MHz AC input signal,combined with a DC signal equivalent to the breakdown voltage of the photodiode, such as to provide the desired oscillation above and below breakdown.

The main issue that arose was the fact that the resistance of the SPAD device is not constant, but will change depending on whether the junction has reached breakdown or not. For this reason, the SPAD was assumed to have two individual resistance values, each one corresponding to the respective state of the device. When the SPAD is below breakdown, only a few tens of microamps are allowed to flow through it, meaning that it's resistance must be extremely high. For the second state of the SPAD, the current through it was expected to achieve a value between a few hundreds of microamperes and a few miliamperes. Thus, since the desired breakdown voltage of the SPAD devices to be used was around 50V, it was safe to assume the maximum and minimum internal resistance of 1MΩ and 100kΩ, respectively.

Now that the load resistance to be applied at the output port of the Bias Tee was determined, the design of the filters was ready to begin. Based on the assumptions mentioned in the previous two paragraphs, the value of the inductor was required to be chosen such that its cut-off frequency, at both the extreme resistance values, should be lower than the frequency of the RF signal. By substituting the values for R (R_SPAD) inside Eq.4.1 and testing for a number of different inductance values L, the optimal value to be applied was calculated as L=200mH.

$$f_c = \frac{L}{2\pi R} \tag{4.1}$$

Continuing, the high pass filter component had to be designed. Thus, the value of the capacitor had to be chosen appropriately to allow this signal through it, but simultaneously attenuate any DC signal coming from the other input port of the Bias Tee. Considering the fact that the only frequency which needs to be cut-off

is that of the DC signal (0Hz), any value of capacitance which provides a cut-off frequency between 0 and 10MHz would be appropriate. To keep the value of the capacitor at a reasonable level and avoid any attenuation of the input signal, C was chosen as $1\mu F$. According to theory, the cut-off frequency of an RC HPF is given by Eq.4.2. Following the same procedure as for the LPF previously, the most suitable value for the capacitance of the HPF was chosen as C=$1\mu F$.

$$f_c = \frac{1}{2\pi RC} \tag{4.2}$$

Fig 4.1 shows the complete schematic of the Bias Tee circuit, including the photodiode, designed to be used in this experiment. The values of the respective components are all indicated on the figure. Further to constructing the circuit in PSpice, Transient Analysis was performed for both the cases of the SPAD being above and below breakdown and the obtained output waveforms are presented in Fig 5.1 and 5.2, respectively.

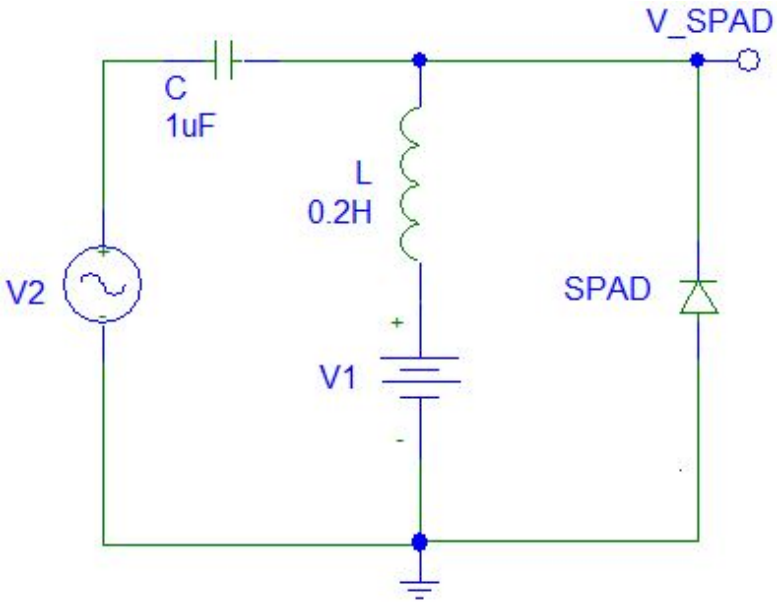

Figure 4.1: Schematic diagram of the quenching circuit designed. The values of the components are also presented.

The circuit shown above was first tested on PSpice to check that it's behaviour was the same as the one expected. Both test cases, for 100kΩ and 1MΩ output resistance, were evaluated. Once this was confirmed, the next step was to proceed

on to testing the circuit in practice. The parts required for this to be achieved were ordered and once received, the Bias Tee circuit was constructed on a breadboard. Next, both input signals where connected to the RF and to the DC ports respectively. The amplitudes of the two signals were scaled down to half so that the output could be conveniently viewed on the oscilloscope. Finally, the circuit's output voltage was tested for both the two values of load resistance and the results were analysed.

4.2.2 Testing of SPADs

In order to proceed with integrating the SPAD devices within the overall design, the first thing to be accomplished was to observe their respective I-V characteristics. For this purpose, a PQC with a ballast resistor of 100kΩ was chosen as the optimal testing circuit. Fig. 4.2 shows the PQC as implemented for the purpose of our experiment. The reason for choosing a 100kΩ quenching resistor, was the fact that, due to the relatively high resistance, even currents of the nA range would produce an unambiguously observable voltage drop across it.

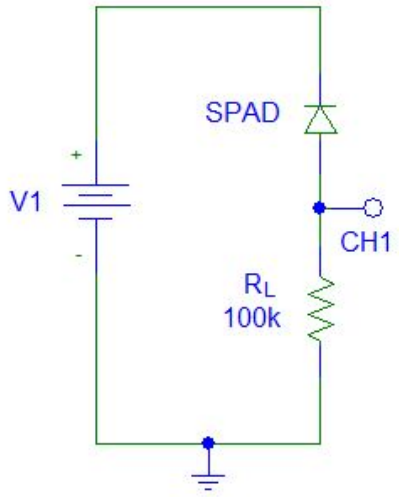

Figure 4.2: Schematic diagram of the testing PQC circuit. R_L is the quenching resistor and the multimeter was connected at CH1 and Ground.

Once the value of the quenching resistor was determined, the circuit was built in practice and a digital multimeter was connected across the two ends of the resistor. Continuing, the active area (eye) of the SPAD device was covered with

black insulating tape, such as to minimise any incident light, which could affect the measurements. Next, the supplied voltage was gradually increased until a detectable voltage drop across the resistor was developed. The value of the supplied voltage, at the specific point where the initial voltage drop was detected, was noted down, which denoted the approximate breakdown voltage (V_B) of the device. The same procedure was repeated for both the two types of photodiodes, as listed in Section 4.1.

$$I_{SPAD} = \frac{V_{R_L}}{R_L} \tag{4.3}$$

For the devices which were identified as to have reached breakdown, a voltage sweep of ± 2V, with steps of 0.1V, around the breakdown point (V_B) was performed. On every step of the sweep, the outputting voltage across the ballast resistor was measured and written down on a table. Once the entire voltage sweep was completed, the produced table described the relation between the supplied voltage (V_S) and the outputting voltage (V_{R_L}). In order to extract the I-V characteristics of the device, it was assumed that the current flowing through the circuit was governed by the value of the ballast resistor. By applying Ohm's law and using the respective equation (shown in Eq.4.3), the current flowing through the SPAD (I_{SPAD}) at each step of the sweep was calculated and the respective I-V characteristics were drawn using an online graph tool.

4.2.3 Development of the LED Circuit and Isolating Box

A 25cm x 20cm x 8cm (length x width x height) Plastic/Polymer box, with a removable top cover, was used to accommodate the quenching and LED circuits. Initially, the entire box was painted with a Matte-Black paint, such that it would reflect as little light as possible. Continuing, 5 holes were drilled on the two short sides of the box (4 on the left, for the inputs, and 1 on the right, for the output) and 4 4mm Banana jacks were placed on the input side, such as to connect the 2 DC power supplies, Ground and Signal Generator inputs, respectively, while a BNC contact was used in the output side, which would later be connected to an oscilloscope. Finally, in order to provide further light insulation for the SPAD, a 2nd, 10cm x 5cm x 7cm internal box was made out of carton and painted Matte-Black, such as to further isolate the SPAD.

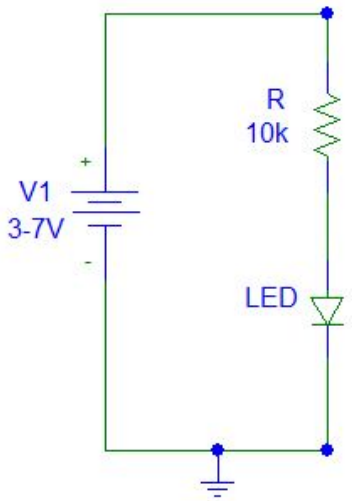

Figure 4.3: Schematic diagram of the designed LED circuit.

In the next step of the process, the LED circuit, which would provide a controllable light inside the isolating box needed to be developed. One first decision was to use a separate 3-7V variable DC power supply in order to power the LED circuit. The main reason for this was the fact that the intensity of the light coming from the LED, needed to be controllable and having a separate power supply would allow us to vary the supplied voltage, as a means of control. The designed circuit is shown in Fig. 4.3 and is comprised of a bright Green LED, with its cathode connected to a 10kΩ series resistor. The colour of the LED was chosen based on the specification datasheet of the SPADs, which shows a peak in the Sensitivity Spectral Range of both the devices for wavelengths in the range of 500-600nm (bright Green corresponds to a wavelength of approximately 550nm). Finally, the value of the resistor was chosen in practice, by trying out different values of resistance, such that the emitted light would hardly be visible with the naked eye.

4.2.4 PQC implementation and Choice of optimal quenching resistor

In order to be able to quantify the advantages of using the developed Bias-Tee circuit, it was deemed necessary to first determine the optimal performance which can be achieved when using the SPAD within the PQC configuration. Thus, it was highly significant to choose the appropriate value of quenching resistance, such as

to achieve the above mentioned goal.

$$\tau = RC \tag{4.4}$$

For the purpose of the project, the optimal performance was defined in terms of the maximum photon detection rate (frequency). This attribute is mostly dependent upon the overall dead -recharge- time, which in turn is governed by the RC time constant, defined by the internal capacitance of the SPAD (C_{SPAD}) and the value external ballast resistor (R_L). Since the value of the time constant is directly proportional to the value of R_L (as shown in Eq. 4.4), then the overall photon detection rate would be expected to increase, as the value of R_L is being decreased. However, as the resistance is decreased below a specific level, the voltage drop developed across the quenching resistor becomes insufficient to force the SPAD below breakdown, thus decreasing tremendously the overall photon detection rate.

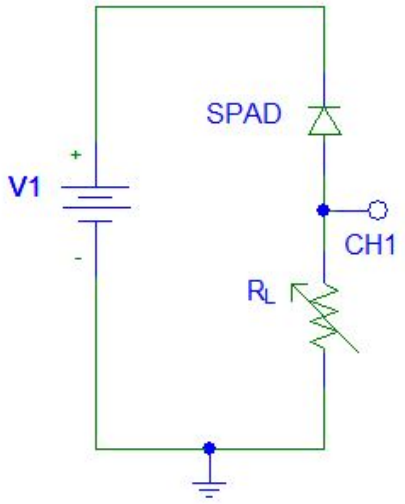

Figure 4.4: Schematic diagram of the second PQC circuit. R_L is a variable resistor and CH1 is connected to the oscilloscope probe.

The circuit used for this experiment is shown in Fig. 4.4, where CH1 was connected to the respective channel of the oscilloscope. Initially, the same 100kΩ resistor was used as the quenching resistor and the supplied voltage (V_A) was set to an excess bias (V_E) of approx. 1.5V above the breakdown voltage V_B. A screenshot of the signal displayed on the oscilloscope was taken and the overall dead-time was calculated. The same procedure was repeated several times, while decreasing the value of the quenching resistor R_L, until it was observed that the output signal

became mostly constant, rather than showing the characteristic avalanche spikes. Finally, the lowest value of quenching resistance, for which the avalanche spikes were unambiguously detectable, was chosen as the optimal one.

4.2.5 Circuit integration, Final Testing and Measurement conduction

The final stage of the project was comprised of integrating all the produced components within the specifically developed isolating box, testing whether the system in its entirety works well altogether and finally conducting measurements to identify the optimal performance which can be achieved by the produced system.

The final integrated circuit, as built within the isolating box, is illustrated in Fig. 4.5. Initially, the quenching resistor R_L was not included within the design, but once the circuit was tested for the first time, the outputting signal was very unstable and no photon detection could be identified. Thus, it was decided that in order to achieve the required results, it was necessary to include one such quenching resistor, which would assist in quenching the avalanche current. The first values of quenching resistance used were identical to those previously used in the conducted tests for the PQC circuit. Gradually, the value of the quenching resistor was decreased and the frequency of the applied AC signal was increased, in order to identify a relation between the two.

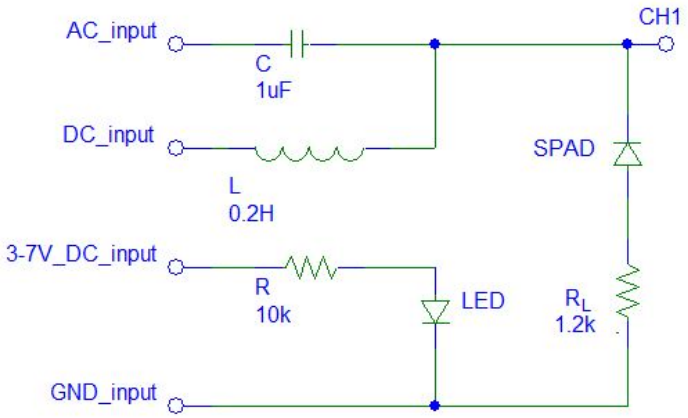

Figure 4.5: Schematic diagram of integrated system which was included within the Isolating box. Each input corresponds to a 4mm banana jack, which were connected to the respective supplies, and the output is a BNC contact going into CH1 of the oscilloscope.

Continuing, it became clear that the overall dead time imposed on the internal PQC had to be smaller than half the period of the modulating AC signal, in order for the system to unambiguously detect photons. Following this observation, the values of the quenching resistance and the frequency of the AC signal were modified constantly, until the signal viewed on the oscilloscope had almost no signs of photons being detected. At each step of the process, screen-shots of the displayed signal were taken and the respective values for R_L and the modulating frequency were noted down. Finally, the limitations of the developed circuit and the previously tested PQC were compared in order to decide on whether the new circuit presented the expected advantages.

Chapter 5

Results

5.1 Bias Tee PSpice Simulation Results[1]

The output signal of the Bias Tee circuit was tested for a load resistance of 100kΩ and 1MΩ, according to the assumptions made during the design stage. Further to constructing the circuit in PSpice, Transient Analysis was performed for both the cases of the SPAD being above and below breakdown and the obtained output waveforms are presented in Fig 5.1 and 5.2, respectively.

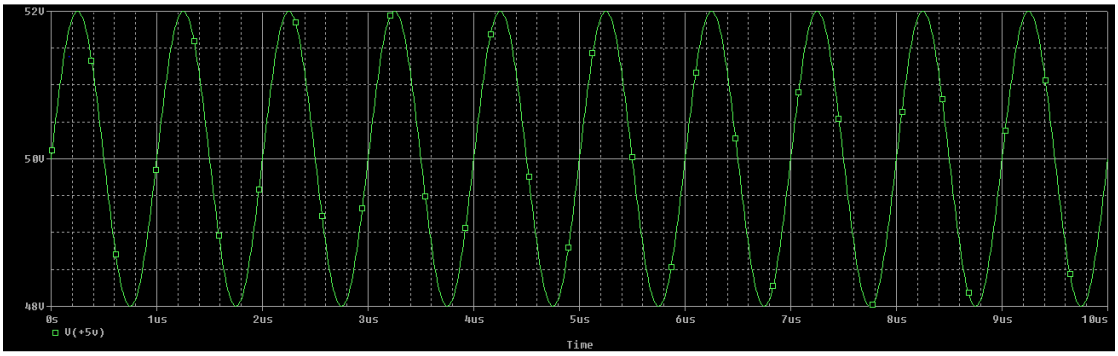

Figure 5.1: First PSpice Transient Analysis performed, having an input signal of 4Vp-p and the approximated resistance to 100kΩ, representing the case where the SPAD is in breakdown, i.e has been triggered.

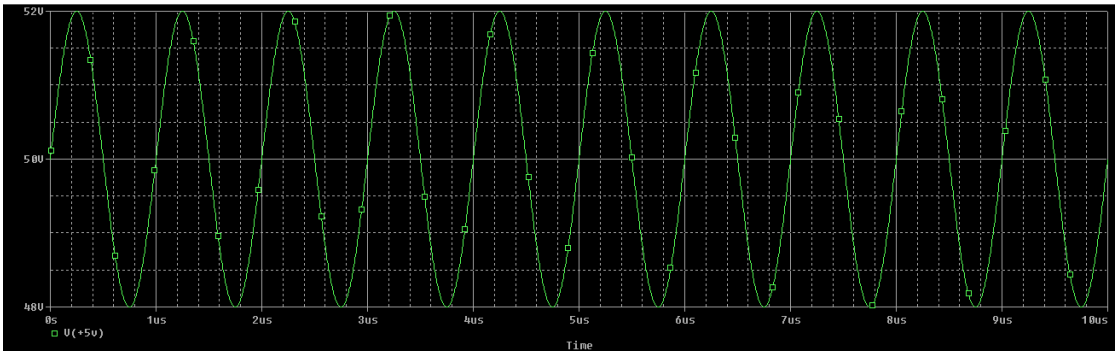

Figure 5.2: Second PSpice Transient Analysis performed, having an input signal of 4Vp-p and the approximated resistance as an open-circuit, representing the case where the SPAD is below breakdown, i.e has not been triggered.

As it can be observed from the PSpice simulations in Figures 5.1, 5.2, there hardly exist any difference between the two assumed states of the SPAD. This fact will ensure that the output voltage supplied at the ports of the SPAD is continuously behaving in the same manner, i.e constantly providing the same waveform voltage, without being dependent upon the current state of the SPAD. Finally, Fig. 5.3 illustrates how the RF current is attenuated and barely has any effect on the current provided by the DC Supply, even for the maximum assumed value of R_SPAD.

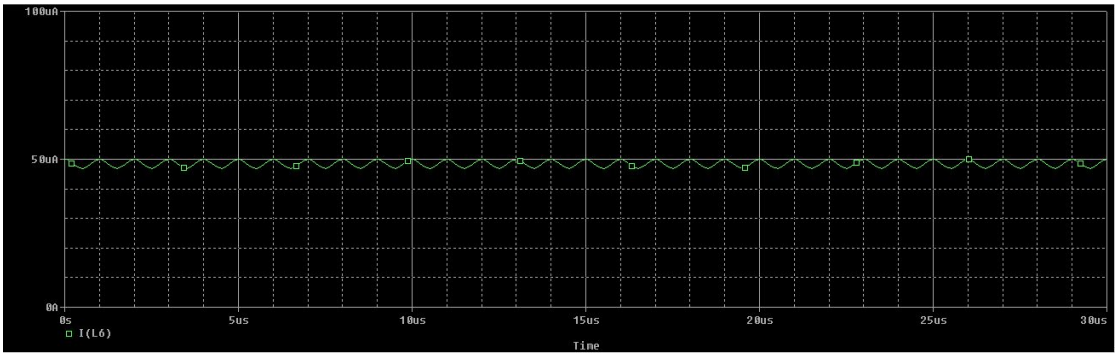

Figure 5.3: PSpice Transient Analysis performed on the current measured at the DC input of the Biast Tee, having connected a load of 1MΩ

5.2 Bias Tee Real Test Results[1]

Once the circuit was simulated on PSpice and it was confirmed, to the extent allowed by the reliability of PSpice, that the circuit would in fact operate as required, it was time to build and test the actual circuit. The signal connected to the RF input came from the function generator and its frequency was set to 1MHz. Both the RF signal and the DC level ware set to half the amplitude used for the PSpice simulations, just to make the output waveform visible on the oscilloscope. Fig. 5.4 shows the input coming from the function generator, while Fig. 5.5 and Fig.5.6 illustrate the output waveforms at a load of 100kΩ and 1MΩ, respectively.

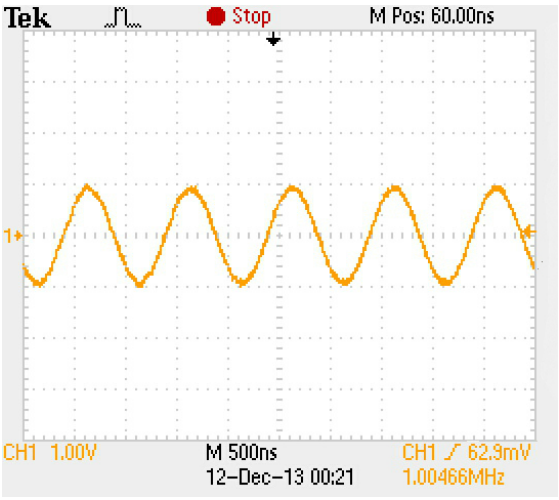

Figure 5.4: Input AC signal measured at the RF port of the Bias Tee

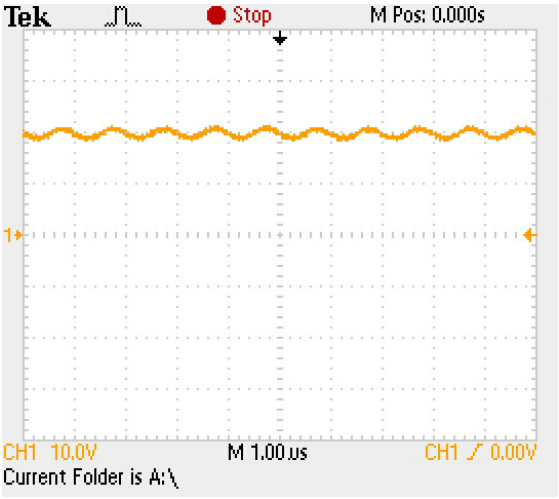

Figure 5.5: Output voltage waveform of the Bias Tee, measured at the RF+DC port with a load of 100kΩ

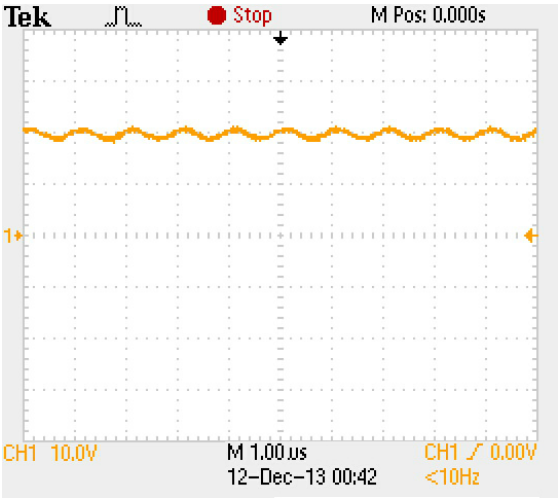

Figure 5.6: Output voltage waveform of the Bias Tee, measured at the RF+DC port with a load of 1MΩ

As can be seen from the figures, the desired circuit behaviour was achieved. For the purpose of the project, the Bias Tee would have to supply an oscillating voltage, above and below breakdown such as to drive the SPAD in and out of its triggering state. Figures 5.5 and 5.5 also show great resemblance to the virtual results received by PSpice. The noise which can be observed withing the later Figures, is created by the function generator itself. Finally, it can be seen again,

that there is hardly any difference between the two figures, meaning that the bias provided by the circuit is not dependent upon the load resistance applied to its output (unless higher values than 10MΩ are used).

5.3 Testing of SPADs Results

Due to voltage supply limitations, each one of the SPAD devices listed in Section 4.1 (Vishay BPW21R and Silonex SLD-70BG), had to be checked in order to determine whether breakdown could actually be reached. The voltage supply which was finally used had a maximum voltage supply of 77V, which could possibly not be sufficient.

Table 5.1: Voltage across load resistor R_L (V_{R_L}) vs Supplied voltage (V_S)

Supplied Voltage (V_S)	Load Resistor Voltage (V_{R_L})
59V	0mV
59.2V	0mV
59.4V	0.6mV
59.6V	10.5mV
59.8V	40mV
60V	80mV
60.2V	140mV
60.4V	210mV
60.6V	310mV
60.8V	440mV
61V	570mV
61.2V	715mV
61.4V	890mV
61.6V	1.06V
61.8V	1.25V
62V	1.46V
62.2V	1.66V
62.4V	1.95V
62.6V	2.3V
62.8V	2.65V
63V	2.9V

Table 5.2: Current through SPAD (I_{SPAD}) vs Supplied voltage (V_S)

Supplied Voltage (V_S)	SPAD Current (I_{SPAD})
59V	0μA
59.2V	0μA
59.4V	0.006μA
59.6V	0.105μA
59.8V	0.4μA
60V	0.8μA
60.2V	1.4μA
60.4V	2.1μA
60.6V	3.1μA
60.8V	4.4μA
61V	5.7μA
61.2V	7.15μA
61.4V	8.9μA
61.6V	10.6μA
61.8V	12.5μA
62V	14.6μA
62.2V	16.6μA
62.4V	19.5μA
62.6V	23μA
62.8V	26.5μA
63V	29μA

The first device to be checked was the Vishay BPW21R. Initially, a draft voltage sweep of the supplied voltage was performed (circuit show in Fig. 4.2), in order to roughly estimate the breakdown voltage (V_B). A significant voltage drop across the load resistor (R_L) was identified for a voltage of approximately 61V. Continuing, a more thorough voltage sweep in the range of 59-63V, with steps of 0.2V was conducted. Table 5.1 shows the directly observed results, illustrating the relation between the supplied voltage and the voltage developed across R_L. Next, the resulting voltage values were converted to the current flowing through the SPAD, using Eq. 4.3 and the resulting calculations can be observed in Table 5.2. Finally, using the values of Table 5.2 and an online graph tool, the I-V characteristics of the device were drawn and are displayed in Fig. 5.7. As can be seen, the actual breakdown voltage of the device was approximately 59.4V, which shows a great deviation from the value of 10V reported within the official documentation of the device[17].

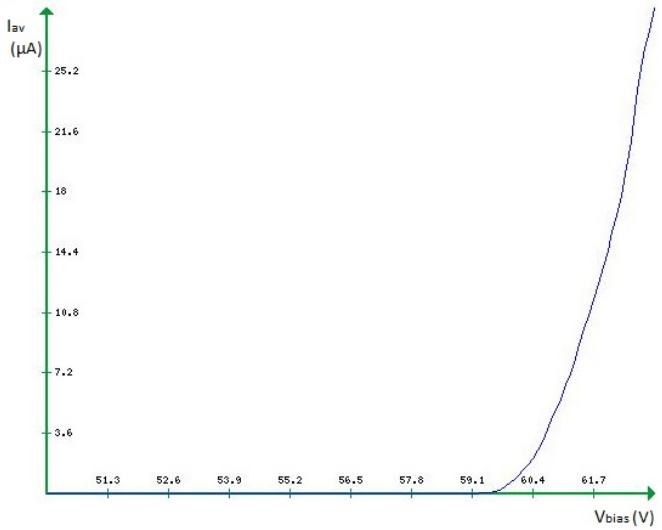

Figure 5.7: Plot of I-V characteristics for Vishay BPW21R

By performing the same draft voltage sweep for a set of Silonex SLD-70BG devices, it was observed that no voltage drop was developed across R_L and, thus, the device did not reach breakdown within the allowed voltage range. Similarly to the first case, the actual breakdown voltage of the device was way beyond the 50V value reported inside it's specification document [18]. For this reason, no further measurements were performed and the device was excluded from all scheduled project experiments.

5.4 Optimal PQC Performance

As mentioned in Section 4.2.4, it was vital to identify the optimal operating point for the PQC, which would later be compared to the one achieved by the finally developed (Bias Tee) system. The starting point for this procedure was to utilize the previously used PQC, including a 100kΩ quenching resistor, and gradually decreasing its value, until signal distortion was observed.

Fig. 5.8, 5.9, 5.10 and 5.11 show screen-shots of the output signal, which was received by supplying 61V to the circuit and having a 100kΩ, 50kΩ, 17.5kΩ and 10kΩ quenching resistors connected, respectively. As can be observed in Fig. 5.8, with the 100kΩ resistor, the average dead-time is approximately 1.5 divisions of the oscilloscope display, which, in practice, is about 150μsec. Thus, the calculated frequency is given as 6.667 kHz.

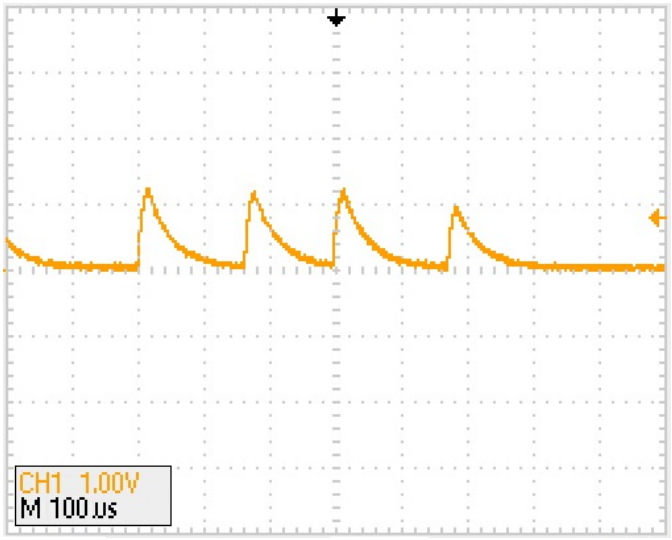

Figure 5.8: Screen-shot of the output signal (V_{R_L}) in the PQC, with R_L=100kΩ. The average photon detection rate was calculated as 6.667 kHz.

Continuing, Fig. 5.9 shows an overall reduction in the duration of the dead time on the detected signals, of approximately 50%. Such an outcome was expected, since there was an equal proportional reduction of the quenching resistance, which has a direct impact to the time-constant of the formed RC circuit. Having an average duration of 3 divisions, with each division corresponding to 25μsec, the photon detection rate of this specific configuration was calculated as 13.334 kHz. Fig. 5.9 also shows some afterpulsing effects, as defined in Section 3.1.3.

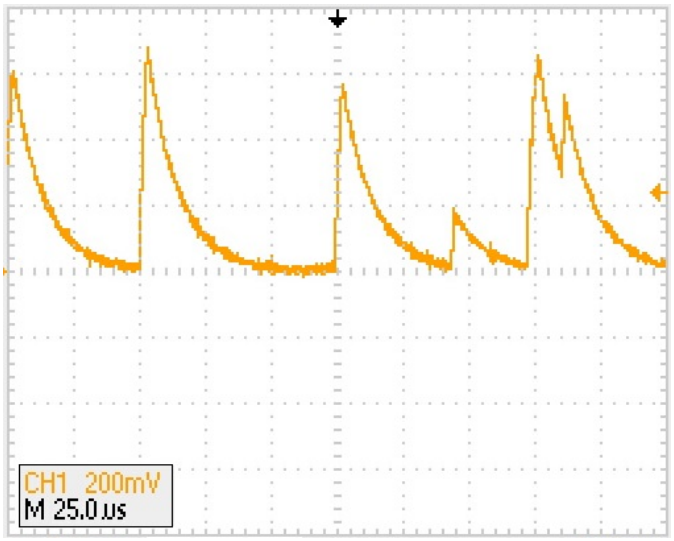

Figure 5.9: Screen-shot of the output signal (V_{R_L}) in the PQC, with R_L=50kΩ. The average photon detection rate was calculated as 13.334 kHz. Afterpulsing can be observed in the last 2 spikes of the figure.

The output received by the optimal value of 17.5kΩ can be observed in Fig. 5.10. Again, having reduced the quenching resistance by an approximate factor of 3, compared to the previous 50kΩ value, the overall dead-time has also been decreased by the same proportion. As witnessed, the duration of the dead time of each spike is approximately 1 division of the oscilloscope display, which corresponds to 25μsec and gives a maximum photon detection frequency of about 40 kHz.

Any further reduction of the quenching resistance R_L would produce output signals similar to the one displayed in Fig. 5.11, where a 10kΩ resistor was used in order to clearly present the distorted signals. As can be witnessed, unlike previous case, the signal does not consist of consecutive avalanche spikes which marks the detection of a photon. On the contrary, a mostly saturated signal can be observed, which corresponds to a continuous avalanche current flowing through the quenching resistor. This happens due to voltage developed across the resistor being insufficient to force the SPAD junction below breakdown. At some stochastic points, this current is eventually quenched, but the overall photon detection rate has been tremendously decreased.

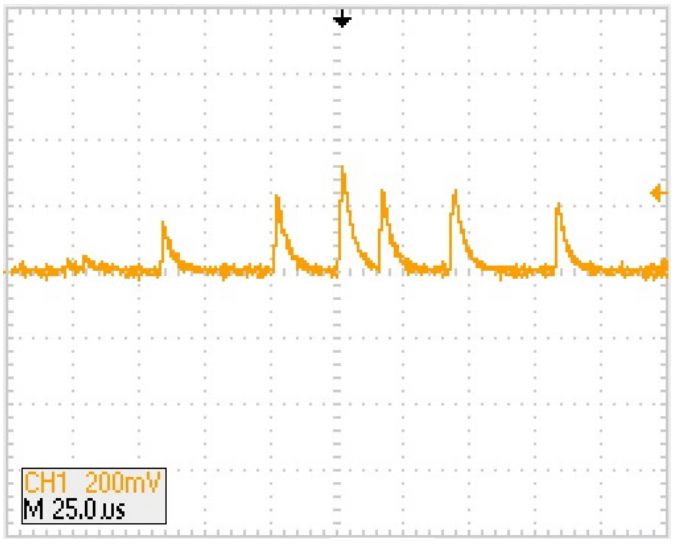

Figure 5.10: Screen-shot of the output signal (V_{R_L}) in the PQC, with R_L=17.5kΩ. The average photon detection rate was calculated as 40 kHz.

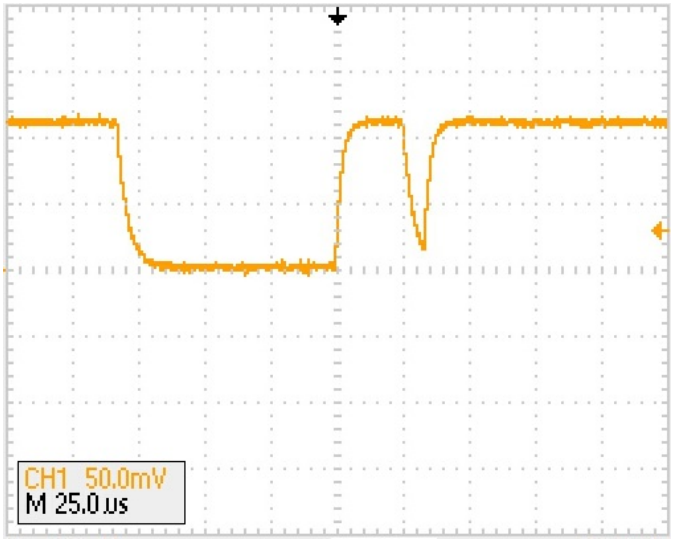

Figure 5.11: Screen-shot of the output signal (V_{R_L}) in the PQC, with R_L=10kΩ. The signal shows a saturated avalanche current flowing through R_L, which is only quenched at random intervals. Photon detection rate cannot be defined in this case.

Finally, Table 5.3 lists the values of quenching resistors R_L together with their respectively observed dead-time and calculated Photon Detection Rate. As can be

seen, the maximum Photon Detection Rate achieved, using the Vishay BPW21R device and the PQC configuration, was 40 kHz.

Table 5.3: Quenching resistors R_L vs Dead-time t_d and Photon Detection Rate (PDR), for each one of the test PQC cases.

Quenching resistance (R_L)	Dead-time (t_d)	Photon Detection Rate (PDR)
100kΩ	150μsec	6.667 kHz
50kΩ	75μsec	13.334 kHz
17.5kΩ	25μsec	40 kHz

5.5 Bias Tee Quenching Circuit Optimum Performance

In order to determine the optimal performance which can be achieved by the developed Bias Tee Quenching circuit, a series of tests were performed in order to identify the maximum frequency of the applied AC signal which can be used, such that detected photons will produce a clearly defined pulse. Fig. 5.12 illustrates the circuit configuration of the tested Bias Tee Quenching Circuit.

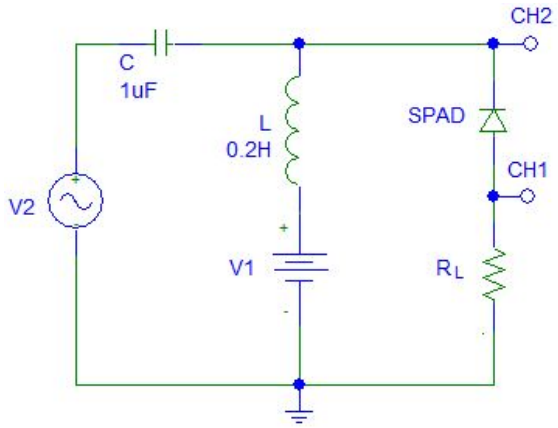

Figure 5.12: Schematic diagram of the experimental Bias Tee Quenching circuit. V2 is the applied AC signal of 4Vp-p and variable frequency and V1 is supplying a DC voltage of 60V. CH1 and CH2 were connected to the respactive channelsof the oscilloscope.

The amplitude of the applied AC signal was set to 4Vp-p, while its frequency (f_{AC}) was varied depending on the value of quenching resistance used. The DC voltage input was set to 60V, which is approximately the breakdown voltage of the specific SPAD device, using or this experiment. Several different values of resistance were tested, starting from the same value used for the PQC tests (100kΩ), but screen-shots of only the maximum and minimum values tested were collected, due to shortage of time. Fig. 5.13 shows the output of the initial test of the circuit, having placed the 100kΩ quenching resistor in series with the SPAD. As can be seen, the maximum applied frequency was 3kHz, which was approximately half the one achieved using the basic PQC configuration. The reason for this is the fact that the device was biased above breakdown only during the positive cycle of the AC signal, thus meaning half of the time. Any major increase of the frequency of the AC signal would eventually disable the device from detecting any photons, since there would not be sufficient time for the avalanche current to be developed.

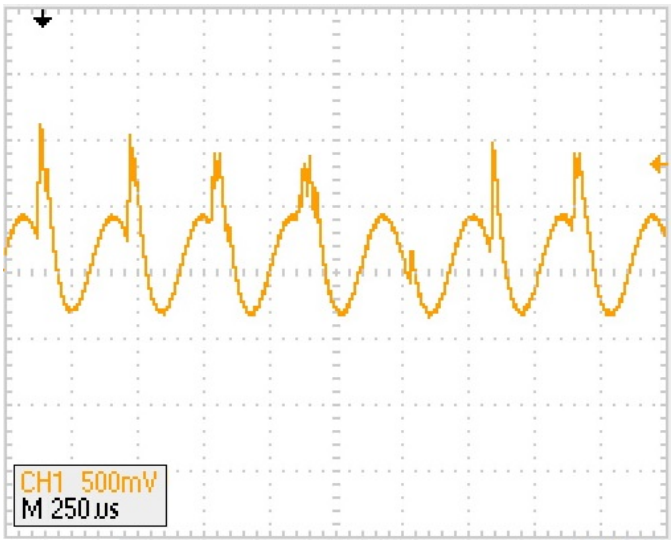

Figure 5.13: Screen-shot of the output signal (V_{R_L}) using the developed Bias Tee quenching circuit, with R_L=100kΩ andf_{AC}=3kHz.

What was observed during the trials was that, as the frequency of the applied AC signal was increased, the value of the quenching resistor, which was placed in series with SPAD, had to be decreased. This was mainly due to the fact that the dead-time of the PQC, which was placed at the output of the Bias Tee, had to be lower than half the period of the applied AC signal, so that there was sufficient time for the avalanche current to be developed and then quenched, during the positive cycle of the signal. This relation is described in Eq. 5.1 below, where t_d is the dead time of the internal PQC and T_{AC} is the period of the applied AC signal.

$$t_d \leq \frac{T_{AC}}{2} \tag{5.1}$$

Within the allowed time of the project, the minimum tested value of quenching resistor, used in the output of the Bias Tee circuit, was 1.8kΩ. During the individual testing of the PQC circuit in Section 5.4, it was observed that the duration of the dead-time was directly proportional to the value of the quenching resistor used and that the measured dead-time, using a 17.5kΩ quenching resistor, was approximately 25μsec. Thus, since the value of 1.8kΩ was approximately 10 times smaller than the 17.5kΩ, it was calculated that the achieved dead time should be roughly 2.5μsec. By applying this value to Eq. 5.1, the minimum period T_{AC} of the applied signal is given as 5μsec and when expressed in terms of frequency, the maximum Photon Detection Rate that can be achieved in theory is given as 200kHz.

Fig. 5.14 shows the output displayed on the screen (V_{R_L}) of the oscilloscope (CH1) and also the intermediate output of the Bias Tee (CH2), having connected the 1.8kΩ quenching resistor, in series with the SPAD, and setting the frequency f_{AC} of the applied AC signal to 200kHz. Despite the fact that the value of the used quenching resistor is much lower than the minimum value used in Section 5.4 (17.5kΩ), the output still shows the characteristic avalanche spikes. This is achieved due to the fact that the voltage across the SPAD junction is not altered solely by the developed voltage across the quenching resistor R_L, but is rather controlled by the applied AC signal.

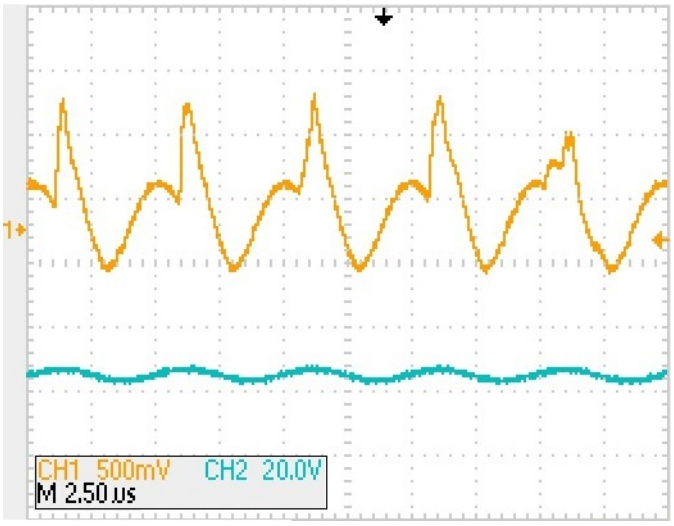

Figure 5.14: Screen-shot of the output signal V_{R_L} (CH1) and the output of the Bias Tee circuit (CH2) using the developed Bias Tee quenching circuit, with R_L=1.8kΩ andf_{AC}=200kHz.

As can be observed in Fig. 5.14, each one of the detected avalanche spikes occurs only after the AC signal has reached it's peak voltage. Generally, the avalanche spikes which occur in all quenching circuits are the result of a swift discharge of the internal capacitor of the SPAD. In this case, as the amplitude of AC signal starts rising, the internal capacitance of the SPAD device is being gradually charged. Once the AC signal reaches it's peak and then begins to fall, the voltage of the charged capacitor becomes bigger than the applied voltage, and thus its charge is quickly discharged within the circuit, producing the avalanche spike.

Chapter 6

Discussion and Conclusions

6.1 General Discussion

From the experimental results received during the course of the project, it was observed that, when using the same quenching resistance in both cases - PQC and BTQC - the PQC offers a higher performance of a factor of 2. However, the limitations set by the quenching resistor in the PQC, have a severe impact on the maximum performance that can be achieved. The developed BTQC helps overcome this particular problem, by allowing very small resistance values to be used, which leads to significant increase of the achievable performance. Comparing the results from Sections 5.4 and 5.5, it is fairly obvious that, when using the developed BTQC, the maximum Photon Detection Rate shows an overall increase by a factor of 5. Even higher performance levels could have been achieved by the developed circuit, if the progress of the project was not interrupted by supply related problems, during the very final days of the project.

Due to the high voltage levels required for the devices to reach breakdown, the power supply needed to be specifically designed to meet the project specification (150V max). The power supply used initially, was a relatively old and used model, which had been modified by the technicians. The first problem identified with the device was that, rather than supplying a constant DC voltage, the supplied signal contained ripples of approximately 2Vp-p (see Fig. A.2. Having fixed this issue, the same power supply eventually broke down after a period of only two days. A substitute power supply was found from another University Department, which was intended to supply voltages of up to 10kV. However, although many different devices of the same type were tested, they all displayed fluctuations in the supplied

voltage, which were not acceptable for the requirements of the project. In the very end, a suitable power supply was found, which could only supply constant DC voltages up to 77V. Due to the power supply being a vital part of the project, this whole procedure set the project behind by a week's time, during the measurement conduction phase, which was the most critical stage of the project.

6.2 Future work

Quenching of SPAD devices, using a Bias Tee circuit, is a scientific area for which no previous research has been identified. Considering the uniqueness of the project in researching the specific field, there is a great potential for future projects to be based on or to continue the work that has been achieved so far. Following discussions with the supervisor of this project, Dr J. Marsland, if a simulation program could be developed to accurately simulate the behaviour of the designed circuit, then the effects of altering certain attributes of the SPAD, such as the dead space of the device, could be studied and the results received from the project could be verified by the already existing theory. As discussed, the outcome of having one such program in place, and comparing the results from this program with the ones received experimentally, is a topic which has a great potential of being officially published. Additionally, a significant interest was expressed by Dr. Marsland, to create supplementary projects for the next academic year, which would be directly related to the findings of this academic work and could extend the scope of the project. Finally, one potential research field which stems from the outcomes of this project is researching the technologies for producing the developed BTQC integrated and with low cost for commercial use.

6.3 Conclusions

Applications of SPADs have been increasing rapidly over the past few years, spanning across a number of different fields, such as telecommunication and imaging technologies. The sensor performance requirements keep becoming tighter, with higher Photon Detection Rates being one of the most important factors. Passive Quenching circuits have been studied and used extensively over the past century, but there is specific bottleneck related with the maximum performance which can be achieved. The Bias Tee Quenching Circuit presented within this paper has the potential of overcoming the limitations set by standard Passive Quenching Circuits. Comparisons between the achievable Photon Detection Rates of the two

circuits, showed an overall increase in the performance of the developed circuit of a factor of 500%, when using the same SPAD device. Based on these results, the developed circuit has a great potential of replacing PQCs, in a number of different applications.

References

[1] L. Vladimirov, "Measurement of Periodic Photodiode Breakdown - Interim Report," University of Liverpool, Liverpool L69 3GJ, United Kingdom, 2013.

[2] J. Zhang, "Semiconductor optical single-photon detectors," Department of Electrical and Computer Engineering, University of Rochester, NY, 14627 USA.

[3] "Advanced imagers silicon technology." `http://www.ll.mit.edu/mission/electronics/AIT/photoncounting.html`, April 2014.

[4] C. Niclass, M. Gersbach, R. Henderson, L. Grant, and E. Charbon, "A Single Photon Avalanche Diode Implemented in 130-nm CMOS Technology," 2007.

[5] S. Cova, M. Ghioni, A. Lacaita, C. Samori and F. Zappa, "Avalanche photodiodes and quenching circuits for single-photon detection," Dipartimento di Elettronica e Informazionevand Centro di Elettronica Quantistica e StrumentazionevElettronica, Consiglio Nazionale delle Ricerche, Piazza Leonardo, Da Vinci 32, Milano 20133, Italy, 1996.

[6] "Ideal Bias Tee (Closed Form): BIASTEE." `https://awrcorp.com/download/faq/english/docs/Elements/biastee.htm`, April 2014.

[7] D. Renker, "Geiger-mode avalanche photodiodes, history, properties and problems," Paul Scherrer Institute, 5232 Villigen, Switzerland, 2006.

[8] M.A. Karami, H. Yoon and E. Charbon, "Single-Photon Avalanche Diodes in sub-100nm Standard CMOS Technologies," Faculty of EEMSC, Delft University of Technology, Netherlands, 2003.

[9] A. Eisele, R. Henderson, B. Schmidtke, T. Funk, L. Grant, J. Richardson and W. Freude, "185 MHz Count Rate, 139 dB Dynamic Range Single-Photon Avalanche Diode with Active Quenching Circuit in 130 nm CMOS Technology," 2011.

[10] V. Savuskan, M. Javitt, G. Visokolov, I. Brouk and Y. Nemirovsky, "Selecting Single Photon Avalanche Diode (SPAD) Passive-Quenching Resistance: An Approach," 2013.

[11] D.A. Ramirez, M.M. Hayat, G.J. Rees and M.A. Itzler, "Model for Passive Quenching of SPADs," 2010.

[12] D.A. Ramirez, M.M. Hayat, G.J. Rees, X. Jiang and M.A. Itzler, "New perspective on passively quenched single photon avalanche diodes: effect of feedback on impact ionization," 2012.

[13] F. Zappa, M. Ghioni, S. Cova, C. Samori and A.C. Giudice, "An integrated active-quenching circuit for single-photon avalanche diodes," Dipartimento di Elettronica e Inf., Politecnico di Milano, Italy, 2002.

[14] R. Boskovi, "Active quenching circuit for single-photon detection with Geiger mode avalanche photodiodes.," Institute, Bijenicka 54, P.O.B. 180, HR-10002 Zagreb, Croatia, 2009.

[15] C. Baylis, L.P. Dunleavy and W. Clausen, "Design of Bias Tees for a Pulsed-Bias, Pulsed-RF Test System using Accurate Component Models," University of South Florida Tampa, FL, 2006.

[16] B. Hicks and B. Erickson, "Bias-T Design Considerations for the LWA," 2008.

[17] Vishay Semiconductors, "BPW21R Silicon Photodiode." `http://www.vishay.com/docs/81519/bpw21r.pdf`, April 2014.

[18] Silonex Inc., "SLD-70BG2 Infrared Rejection Filter Planar Photodiode." `http://www.farnell.com/datasheets/16350.pdf`, April 2014.

Appendices

Appendix A

Section 1 : Figures

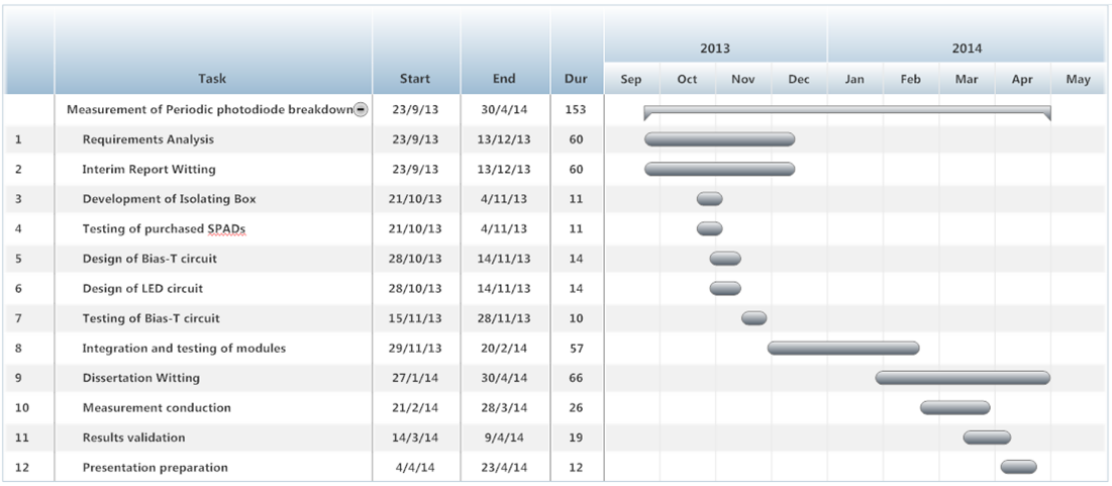

	Task	Start	End	Dur
	Measurement of Periodic photodiode breakdown	23/9/13	30/4/14	153
1	Requirements Analysis	23/9/13	13/12/13	60
2	Interim Report Witting	23/9/13	13/12/13	60
3	Development of Isolating Box	21/10/13	4/11/13	11
4	Testing of purchased SPADs	21/10/13	4/11/13	11
5	Design of Bias-T circuit	28/10/13	14/11/13	14
6	Design of LED circuit	28/10/13	14/11/13	14
7	Testing of Bias-T circuit	15/11/13	28/11/13	10
8	Integration and testing of modules	29/11/13	20/2/14	57
9	Dissertation Witting	27/1/14	30/4/14	66
10	Measurement conduction	21/2/14	28/3/14	26
11	Results validation	14/3/14	9/4/14	19
12	Presentation preparation	4/4/14	23/4/14	12

Figure A.1: Gantt Chart of the predicted progress of the project at the beggining of the year

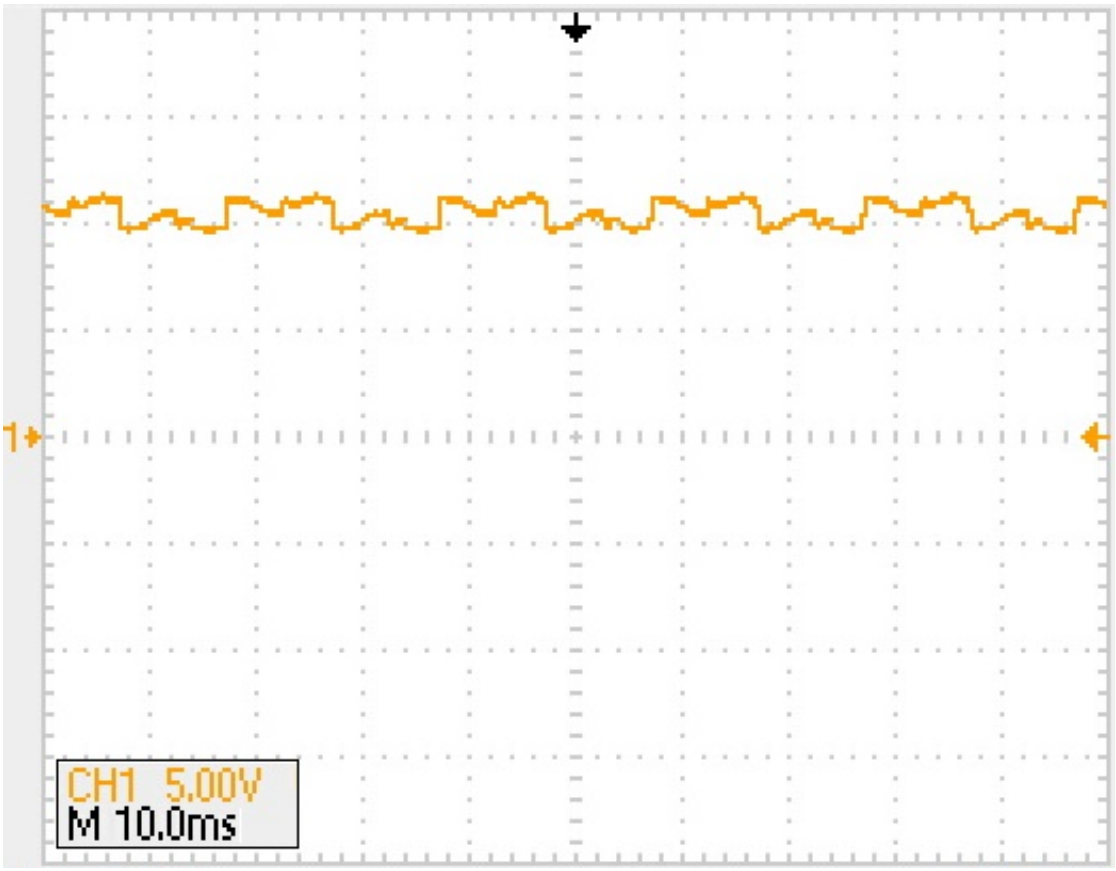

Figure A.2: Screen-shot of the observed ripples in the output o the initially used DC power supply.